Atmos. Chem. Phys. Discuss., 12, 20745–20783, 2012
www.atmos-chem-phys-discuss.net/12/20745/2012/
doi:10.5194/acpd-12-20745-2012

Atmospheric Chemistry and Physics Discussions

CCN activity and volatility of β-caryophyllene secondary organic aerosol

M. Frosch[1,*], M. Bilde[1], A. Nenes[2,3], A. P. Praplan[4], Z. Jurányi[4,], J. Dommen[4], M. Gysel[4], E. Weingartner[4], and U. Baltensperger[4]**

[1]Department of Chemistry, University of Copenhagen, Denmark
[2]School of Earth & Atmospheric Sciences, Georgia Institute of Technology, Atlanta, GA, USA
[3]School of Chemical and Biomechanical Engineering, Georgia Institute of Technology, Atlanta, GA, USA
[4]Laboratory of Atmospheric Chemistry, Paul Scherrer Institute, Villigen, Switzerland
[*]now at: Division of Nuclear Physics, University of Lund, Sweden
[**]now at: School of Engineering, Institute of Aerosol and Sensor Technology, University of Applied Sciences Northwestern Switzerland, Windisch, Switzerland

Received: 4 July 2012 – Accepted: 4 August 2012 – Published: 17 August 2012

Correspondence to: M. Frosch (mia.frosch@nuclear.lu.se)

Published by Copernicus Publications on behalf of the European Geosciences Union.

Abstract

In a series of smog chamber experiments, the Cloud Condensation Nuclei (CCN) activity of Secondary Organic Aerosol (SOA) generated from ozonolysis of β-caryophyllene was characterized by determining the CCN derived hygroscopicity parameter, κ_{CCN}, from experimental data. Two types of CCN counters, operating at different temperatures, were used. The effect of semi-volatile organic compounds on the CCN activity of SOA was studied using a thermodenuder.

Overall, SOA was only slightly CCN active (with κ_{CCN} in the range 0.001–0.16), and in dark experiments with no OH scavenger present, κ_{CCN} decreased when particles were sent through the thermodenuder (with a temperature up to 50 °C).

SOA was generated under different experimental conditions: in some experiments, an OH scavenger (2-butanol) was added. SOA from these experiments was less CCN active than SOA produced in experiments without an OH scavenger (i.e. where OH was produced during ozonolysis). In other experiments, lights were turned on, either without or with the addition of HONO (OH source). This led to the formation of more CCN active SOA.

SOA was aged up to 30 h through exposure to ozone and (in experiments with no OH scavenger present) to OH. In all experiments, the derived κ_{CCN} consistently increased with time after initial injection of β-caryophyllene, showing that chemical ageing increases the CCN activity of β-caryophyllene SOA. κ_{CCN} was also observed to depend on supersaturation, which was explained either as an evaporation artifact from semi-volatile SOA (only observed in experiments lacking light exposure) or, alternatively, by effects related to chemical composition depending on dry particle size.

Using the method of Threshold Droplet Growth Analysis it was also concluded that the activation kinetics of the SOA do not differ significantly from calibration ammonium sulphate aerosol.

1 Introduction

Aerosol particles play an important role in global climate both by interacting directly with solar radiation and through their ability to take up water and form cloud droplets, i.e. act as Cloud Condensation Nuclei (CCN). The latter is referred to as the indirect aerosol effect (IPCC, 2007). The ability of particles to act as CCN depends on their size and chemical composition. Radiative properties of clouds are influenced by the size and number concentration of the individual cloud droplets, which is a function of the amount of water available and the number concentration of CCN.

Atmospheric aerosol particles are composed of inorganic as well as organic compounds. In many locations, organic material comprises a significant fraction (up to 90 %) of the total aerosol mass (Kanakidou et al., 2005; Jimenez et al., 2009). The organic components are introduced either through primary emissions or as secondary material. Secondary organic aerosol (SOA) is created through condensation of products from gas phase oxidation of Volatile Organic Compounds (VOC), which can be of either biogenic or anthropogenic origin. Emissions of VOC are estimated to be more than 1000 $\mathrm{Tg\,C\,yr^{-1}}$, the majority being biogenic (Guenther et al., 1995; Goldstein and Galbally, 2007). The contribution of SOA to the total amount of organic carbon in the aerosol phase is significant (e.g. Kanakidou et al., 2005; Goldstein and Galbally, 2007; Hallquist et al., 2009), but has a strong seasonal dependency (Kleindienst et al., 2007). Monoterpenes, such as α-pinene, are among the most important biogenic SOA precursors (Kanakidou et al., 2005). The contribution of sesquiterpenes, such as β-caryophyllene, to the total VOC emissions is smaller (Griffin et al., 1999), but due to high aerosol yields from sesquiterpene oxidation, their contribution to SOA can be significant (e.g. Griffin et al., 1999; Sakulyanontvittaya et al., 2008).

Products from oxidation of β-caryophyllene have been the focus of previous studies (e.g. Jaoui et al., 2003; Lee et al., 2006; Chan et al., 2011), showing that both the aerosol yield and physical properties, such as hygroscopicity and CCN activity, of SOA depend strongly on experimental conditions (Donahue et al., 2005; Huff-Hartz et al., 2005; Asa-Awuku et al., 2009; Alfarra et al., 2012; Tang et al., 2012). For example, the aerosol yield from photo-oxidation of β-caryophyllene is much greater than the yield from ozonolysis without light exposure (Hoffmann et al., 1997; Griffin et al., 1999), indicating that increased levels of OH during photolysis favor production of low-volatility species. As another example, SOA generated in the presence of an OH scavenger (2-butanol) has a much lower CCN activity than SOA generated in the presence of OH (Asa-Awuku et al., 2009; Tang et al., 2012).

Compared to SOA from other terpenes, CCN activity of SOA from β-caryophyllene is quite low. The CCN-derived hygroscopicity parameter κ (Petters and Kreidenweis, 2007; see also Sect. 2) for β-caryophyllene SOA is < 0.05 (Huff-Hartz et al., 2005; Asa-Awuku et al., 2009; Alfarra et al., 2012), which for example is lower than the CCN derived κ of ~ 0.1 which has been reported for α-pinene (e.g. Prenni et al., 2007; Duplissy et al., 2008; Jurányi et al., 2009; Frosch et al., 2011). However, CCN activity of β-caryophyllene SOA from smog chamber experiments is reported to depend on the initial precursor concentration, being higher for lower concentrations (Tang et al., 2012), similar to the findings for α-pinene SOA (e.g. Duplissy et al., 2008). Since sesquiterpenes contain one more isoprene unit than monoterpenes, oxidation products of sesquiterpenes generally have a higher number of carbon atoms and a higher molar mass. Based on this, SOA from oxidation of β-caryophyllene is expected to be of higher average molar mass with a lower oxygen-to-carbon ratio and therefore also less water soluble and less CCN active than SOA from monoterpenes (Huff-Hartz et al., 2005).

Asa-Awuku et al. (2009) studied CCN activity of β-caryophyllene SOA using two different CCN Counters (CCNC) and found that CCN activity was greater when measured with a Static Diffusion (SD) CCNC than when measured with a continuous flow (CF) CCNC. This difference was related to the different operating temperatures in the two instruments: the SD-CCNC operated close to room temperature, whereas the temperature in the CF-CCNC was above room temperature, the degree of which depended on the supersaturation. It was recently shown that β-caryophyllene SOA contains volatile or semi-volatile material (Asa-Awuku et al., 2009; Tang et al., 2012), which at elevated temperature may evaporate from the particles passing through the heated growth chamber of the CF-CCNC, and that the residual components were not only less volatile but also less hygroscopic than the evaporated fraction (Asa-Awuku et al., 2009). Relations between volatility and hygroscopicity of SOA produced in smog chambers have been examined by e.g. Tritscher et al. (2011), who suggested that simultaneous increases in volatility and hygroscopicity were the result of fragmentation of oxidation products, resulting in highly functionalized species with low molecular weight.

The connections between volatility and CCN activity of SOA have been the focus of previous studies, e.g. by Kuwata et al. (2011) who used a Thermodenuder (TD) to study volatility effects of SOA produced from ozonolysis of α-pinene in a continuous-flow chamber at different steady-state organic particle mass concentrations (M_{org}, in the range 1.4–37 $\mu\text{g}\,\text{m}^{-3}$). They found that while chemical composition (characterized by oxygen-to-carbon and hydrogen-to-carbon ratios, measured with aerosol mass spectrometry) depended solely on the post-TD M_{org}, the behavior of CCN activity was more complex. At room temperature, CCN activity was independent of M_{org}, with κ values of approximately 0.1. However, after passing particles through a TD with an elevated temperature (100 °C), CCN activity decreased with increasing M_{org}. A hypothesis to explain these observations was an increased fraction of oligomers in the particles. This increase was attributed partially to evaporation of high-volatility monomers and partially to particle-phase reactions favored at high values of M_{org}. For example, reactions such as aldol condensation, acid dehydration and hemiacetal formation, resulting in products with higher molar mass than the reactants, are favored in a warm TD, due to higher reaction rates at elevated temperatures (Jang and Kamens, 2001; Gao et al., 2004; Kuwata et al., 2011). Thus, as also observed by Tritscher et al. (2011), fragmentation is not the only chemical process responsible for changes in volatility and hygroscopicity. Oligomerization and changes in functionalization also affect the physical properties of SOA.

The less volatile material in β-caryophyllene SOA has been found to impact droplet growth kinetics (Asa-Awuku et al., 2009), possibly a consequence of soluble material evaporating from the particle surface and a redistribution of amorphous, “waxy” material in the surface of the activating droplet. Variations in droplet growth kinetics were related to the fraction of water-soluble organic material, which – combined with the semi-volatile fraction of β-caryophyllene SOA – could have several atmospheric implications (Nenes et al., 2001; Raatikainen et al., 2012). For example, the semi-volatile material could evaporate from particles with delayed water uptake and activation during warm days, causing a diurnal variation in CCN activity (Asa-Awuku et al., 2009).

In this work, CCN activity and volatility of SOA from β-caryophyllene are characterized in a series of smog chamber experiments. Particles were generated under different experimental conditions: ozonolysis with or without an OH scavenger, and ozonolysis under light exposure with an increased OH level from ozone photolysis. Additionally, some experiments were conducted with a strong OH source (photolysis of HONO). In all experiments, the initial concentration of β-caryophyllene was 25 ppb. Similar to the strategy of Asa-Awuku et al. (2009), CCN activity was determined with two different CCN counters operating at different temperature. Connections between volatility, CCN activity and OH exposure were explored with a TD. Finally, droplet activation kinetics was explored using CCN activation measurements.

2 Theory

The equilibrium supersaturation of water (SS) for an aqueous solution droplet with known size and chemical composition can be determined using the Köhler equation (Köhler, 1936). Here we express it in the following way (Seinfeld and Pandis, 2006),

$$\mathrm{SS} = \frac{p}{p_0} - 1 = a_\mathrm{w} \cdot \exp\left(\frac{4 v_\mathrm{w} \sigma_\mathrm{al}}{RT D_p}\right) - 1 \quad (1)$$

where a_w is the water activity, v_w is the partial molar volume of water, approximated with the ratio of the molar mass, M_w, to the density, ρ_w, of water, σ_{al} is the air-liquid surface tension, R is the ideal gas constant, T is absolute temperature, and D_p is droplet diameter. The maximal SS in dependence of D_p defines the so-called critical supersaturation, SS_c.

Several one-parameter approaches exist to describe the concentration dependence of water activity and thereby the relationship between dry particle size and water uptake, for example the effective number of moles of soluble ions or non-dissociating molecules per dry particle volume (Rissler et al., 2006) or the ionic density ρ_{ion} (Wex et al., 2007). Here we apply the widely used hygroscopicity parameter, κ, introduced by Petters and Kreidenweis (2007),

$$\frac{1}{a_w} = 1 + \kappa \frac{V_s}{V_w} \tag{2}$$

where V_s is the solute volume (assumed to be dry particle volume) and V_w is the water volume. The most hygroscopic species found in ambient aerosols (NaCl) have a maximum κ of ~ 1.3, whereas $\kappa = 0$ indicates that the particle is insoluble in water. Combining Eqs. (1 and 2) yields the equation defining "κ-Köhler theory" (Petters and Kreidenweis, 2007);

$$SS = \frac{D_p^3 - D_{dry}^3}{D_p^3 - D_{dry}^3(1-\kappa)} \cdot \exp\left(\frac{4 M_w \sigma_{al}}{RT \rho_w D_p}\right) - 1 \tag{3}$$

where D_{dry} is the diameter of the dry particle. κ can be determined from equilibrium growth factors (GF) as well as from critical dry diameters or supersaturations measured at sub- and supersaturated conditions, respectively. The latter is referred to as the CCN derived hygroscopicity parameter, κ_{CCN}.

3 Experimental

3.1 SOA formation from β-caryophyllene

The β-caryophyllene experiments were carried out in May–June 2009 at the Paul Scherrer Institute (PSI) in a 27 m^3 Teflon reaction chamber (described in detail by Paulsen et al., 2005). Twelve ozonolysis experiments were carried out (see Table 1): two experiments in which 2-butanol was added to act as an OH scavenger (a and b), three experiments without addition of an OH scavenger leading to OH radical reactions as long as ozonolysis occurred (c–e); two with lights turned on leading to OH production from ozone photolysis (f and g), and five with lights and the addition of HONO (h–l) as an efficient OH source. No seed aerosol was used. The smog chamber is placed inside a temperature-controlled wooden enclosure kept at approximately 20 °C, slightly below ambient temperature outside this enclosure (24–30 °C).

Initially, the chamber was cleaned by flushing with ozone for 3–5 h and then with purified air (flow rate approximately 150 $\mathrm{l\,min^{-1}}$) for at least 24 h. During experiments, the chamber was first humidified to a relative humidity of 5–10 % before introducing first ozone and then β-caryophyllene (> 98.5 %, Fluka). Ozone generation is described by Paulsen et al. (2005); the initial concentration of ozone was 300 ppb. In experiments a and b, 0.22 ml 2-butanol (corresponding to ~ 2 ppm) was added by placing it in a glass sampling bulb and letting it evaporate by heating to 80 °C. The vapor was then flushed into the chamber with purified air. 6.3 µl β-caryophyllene was added in the same way, resulting in an initial concentration of 25 ppb. After injection of β-caryophyllene, measurements were carried out for up to 30 h.

In experiments f–l, solar light was simulated with four xenon arc lamps (total 16 kW rated power), which were turned on at the same time as β-caryophyllene was injected. In spite of active cooling in the wooden enclosure, this typically caused the smog chamber temperature to rise to approximately 25 °C. Furthermore, in experiments h–l, OH was generated through photolysis of HONO, which was added continuously with a system designed according to Taira and Kanda (1990). Injection of HONO began at least 60 min before lights were turned on.

3.2 Instruments

Particle generation and growth was monitored with a Scanning Mobility Particle Sizer (SMPS) composed of a differential mobility analyzer (DMA, TSI 3071) and a condensation particle counter (CPC, TSI 3010). CCN activity of SOA was characterized with two CCN counters: one was a continuous-flow streamwise thermal-gradient CCN counter (CF-CCNC from DMT, CCNC-100, described by Roberts and Nenes, 2005 and Lance et al., 2006); the other was a static diffusion thermal-gradient CCN counter (SD-CCNC from University of Wyoming, Model 100B; described by Bilde and Svenningsson 2004; Snider et al., 2006, 2010; Svenningsson and Bilde, 2008).

The CCN counters were used to determine the size-dependent critical supersaturation (SS_c) for a known dry particle size or the critical dry diameter ($D_{dry,c}$) at a known supersaturation. Particles leaving the smog chamber were sent through a neutralizer and a DMA (custom-built, equivalent to TSI, 3071) which operated with an aerosol to sheath flow ratio of 1 : 10 to ensure a narrow size distribution. The DMA selected a quasi-monodisperse sample flow with a known diameter (D_{dry}), and varied in steps between different diameters. The flow leaving the DMA was then split between a CPC (TSI 3022A) and the two CCN counters. In the CF-CCNC, $D_{dry,c}$ was determined for various constant values of SS. This was also done in the SD-CCNC, but during some experiments, SS_c was instead determined for known values of D_{dry}. Here supersaturation was varied in the range 0.05–2 %, and SS_c was determined for a given D_{dry}.

The CPC draws a flow of 0.3 $\mathrm{l\,min^{-1}}$; the CF-CCNC 0.5 $\mathrm{l\,min^{-1}}$ and the SD-CCNC 3 $\mathrm{l\,min^{-1}}$. The sheath flow in the DMA was 8 $\mathrm{l\,min^{-1}}$. To obtain a sample to sheath flow ratio of 1 : 10, dilution of the sample flow after the DMA was necessary. This was done by sending the exhaust from the SD-CCNC (3 $\mathrm{l\,min^{-1}}$) through a diffusion drier and a particle filter and adding it to the flow of 0.8 $\mathrm{l\,min^{-1}}$ exiting the DMA. It was assumed that the chemical composition of the gas phase in the exhaust of the SD-CCNC was similar to the gas phase of the flow coming directly from the smog chamber, and that dilution therefore did not alter the partitioning between particles and the gas phase in the aerosol flow. The dilution system was used during the fraction of each experiment when the SD-CCNC was running (up to eight hours in experiments lasting up to 30 h). Turning off the SD-CCNC and disconnecting the dilution system did not change the fraction of activated particles, i.e. the ratio between the number concentration of activated particles (measured with the CCNC) and the total number concentration (measured with the CPC). To avoid a high level of doubly charged particles, the selected diameters were mainly chosen to be above the mode of the size distribution in the smog chamber. $D_{\mathrm{dry,c}}$ and $\mathrm{SS_c}$ were determined by correcting for doubly charged particles and fitting the activated fraction as a function of dry particle diameter or supersaturation, respectively, to a sigmoidal function, similar to the approach of e.g. Prisle et al. (2008).

The CCN counters were calibrated using dry Ammonium Sulphate (AS) particles; measurements for the calibration curves were obtained both before and during the two months of smog chamber experiments.

The Optical Particle Counter (OPC) of the CF-CCNC measures droplet size and can therefore describe growth kinetics of activating particles. For a given mass transfer coefficient, activated CCN will grow to droplets of similar diameter (D_{OPC}) if exposed to the same supersaturation. Some organic compounds can delay or even hinder growth kinetics (e.g. Nenes et al., 2001; Asa-Awuku and Nenes, 2007; Sjogren et al., 2007; Asa-Awuku et al., 2009). This effect is evaluated by comparing D_{OPC} of activated SOA to activating ammonium sulphate particles characterized at the same critical supersaturation and under identical conditions of instrument operation (similar to the approach of e.g. Engelhart et al., 2008; Asa-Awuku et al., 2009, 2010). This technique is also referred to as Threshold Droplet Growth Analysis (TDGA). Since the CCN activity of ammonium sulphate in general is different from the CCN activity of SOA, the dry diameter of ammonium sulphate particles activating at a given supersaturation is different from the dry diameter of SOA activating at the same supersaturation, but if CCN experiments are carried out under identical conditions of instrument operation the activated droplets will grow to the same size when detected by the OPC. The aim was therefore not to report the actual size of the activated particles, but to detect any differences between activated SOA and ammonium sulfate particles. Time resolution for the CF-CCNC was 1 s, but to increase accuracy dry particle size and supersaturation were kept constant for at least one minute, and D_{OPC} was averaged over this time period. Unweighted standard deviations were also determined in this way. D_{OPC} for ammonium sulphate particles at different supersaturations obtained during calibration measurements on different days are shown in Fig. 1.

Special attention was given to the concentration of CCN in the CF-CCNC to prevent vapor depletion affecting the size of activated droplets (Lathem and Nenes, 2011; Raatikainen et al., 2012). In all smog chamber experiments, the number concentration of CCN was below 2500 cm^{-3}, which does not significantly influence the level of supersaturation in the instrument or activated droplet size (Lathem and Nenes, 2011).

During some parts of the experiments, a thermodenuder (TD) consisting of a heater and an activated charcoal denuder (Burtscher et al., 2001) was inserted directly outside the smog chamber (before the particles entered the neutralizer and the DMA). The temperature of the TD was either ambient temperature (in the range 24–30 °C), 35 °C or 50 °C. The heated section of the TD had an inner diameter of 2 cm and a length of 50 cm. The flow through the TD was 0.8 $\mathrm{l\,min}^{-1}$ in all experiments, corresponding to a residence time in the heated section of 6.2 s. This is slightly shorter than the residence time in the growth chamber of the CF-CCNC (~ 8 s). The importance of a sufficiently long residence time to establish equilibrium between the gas and particle phases for quantitative studies of evaporation rates has been addressed by e.g. Riipinen et al. (2010). In the present study, however, the TD was used to study if a qualitative correlation between volatility and CCN activity could be determined for SOA.

Particles are lost in a TD due to different processes, e.g. Brownian diffusion, and sedimentation (Burtscher et al., 2001). The magnitudes of these losses depend on flow rate and particle size and were estimated by comparing the particle number concentration when the TD was bypassed to the number concentration when particles went through the TD without any heating. This transmission was 80–90 % in the presented experiments (not including effects of thermophoresis).

4 Results and discussion

Results from SMPS scans from individual experiments are shown in Fig. 2. Figure 2a shows the total number concentration as a function of time after initial injection of β-caryophyllene, and Fig. 2b shows the mean dry particle diameter as a function of time after injection of β-caryophyllene. In the four types of experiments, OH levels gradually increased (see Table 1). OH concentration was minimal during experiments a and b, i.e. with OH scavenger. During experiments without an OH scavenger (experiments c–e), OH was generated during ozonolysis, and OH levels were higher during experiments with lights on, either with or without the addition of an OH source (i.e. photolysis of HONO).

After nucleation, the total number concentration decreased as a function of time due to coagulation and wall losses in the smog chamber. Similar total number concentrations were obtained during all four types of experiments (Fig. 2a), but experiments carried out with lights on and the addition of HONO in general resulted in larger particles (Fig. 2b).

4.1 CCN activity of particles generated in dark experiments

Two types of experiments were carried out with lights off (experiments a–e, see Table 1). In two of these experiments, 2-butanol was added to act as an OH scavenger (experiments a and b). Figure 3a shows the critical diameter $D_{\mathrm{dry,c}}$ of SOA (at 0.60–1.51 % supersaturation) for these two types of experiments. To ease comparison between results from different supersaturations, κ_{CCN} is shown in Fig. 3b. All CCN measurements displayed in Fig. 3 were performed with the CF-CCNC.

In experiments with an OH scavenger (experiments a and b), the generated particles did not activate at supersaturations below 1.3 % for the several hours after nucleation. Therefore, $D_{\mathrm{dry,c}}$ was only determined at SS = 1.32 and 1.51 %, shown in Fig. 3. κ_{CCN} was in the range 0.001–0.005. For both supersaturations, a temporal trend was observed: the CCN activity decreased linearly with time (from to 163 nm to 124 nm over 17 h, with a rate of $3.0 \pm 0.2\,\mathrm{nm\,h^{-1}}$ for SS = 1.32 %, and from 140 nm to 102 nm with a rate of $2.8 \pm 0.14\,\mathrm{nm\,h^{-1}}$ for SS = 1.51 %, see Table 2). This is in quantitative agreement with the findings of Asa-Awuku et al. (2009), who at SS = 1.02 % observed a linear decrease in $D_{\mathrm{dry,c}}$ in the range 70–90 nm of $3.0\,\mathrm{nm\,h^{-1}}$, and at SS = 0.61 % observed a linear decrease in the range 115–130 nm of $2.0\,\mathrm{nm\,h^{-1}}$ (corresponding to κ_{CCN} in the range 0.017–0.040) over a period of approximately 10 h for particles generated in absence of OH. Huff-Hartz et al. (2005) reported $D_{\mathrm{dry,c}} = 152 \pm 26$ nm at SS = 1 % of particles generated from ozonolysis of β-caryophyllene in the presence of 2-butanol. This corresponds to $\kappa_{\mathrm{CCN}} = 0.004$, which is less CCN active than SOA studied by Asa-Awuku et al. (2009), but in good agreement with the findings of the present study.

Particles generated in the presence of OH (experiments c–e) were significantly more CCN active and also showed an increase in κ_{CCN} as a function of time. In the present study, the CCN activity was studied at three different supersaturations: at SS = 0.60 %, $D_{\mathrm{dry,c}}$ decreased from 115 nm to 94 nm ($\kappa_{\mathrm{CCN}} = 0.029$–$0.043$) over 6.5 h corresponding to $3.3 \pm 0.3\,\mathrm{nm\,h^{-1}}$ and at SS = 1.02 %, $D_{\mathrm{dry,c}}$ decreased from 78 nm to 69 nm ($\kappa_{\mathrm{CCN}} = 0.026$–$0.048$) over 10 h, corresponding to $0.85 \pm 0.9\,\mathrm{nm\,h^{-1}}$ (see also Table 2). Asa-Awuku et al. (2009) determined $D_{\mathrm{dry,c}}$ at the same two supersaturations and observed a $D_{\mathrm{dry,c}}$ in the range 105–130 nm (corresponding to $\kappa_{\mathrm{CCN}} = 0.018$–$0.038$) and a decrease of $2.6\,\mathrm{nm\,h^{-1}}$ over approximately 10 h for SS = 0.61 %; for SS = 1.02 % $D_{\mathrm{dry,c}}$ was in the range 65–95 nm ($\kappa_{\mathrm{CCN}} = 0.010$–$0.050$), corresponding to a decrease of $2.8\,\mathrm{nm\,h^{-1}}$. In the present study, $D_{\mathrm{dry,c}}$ is within the same range but slightly lower than reported by Asa-Awuku et al. (2009).

In the present study, $D_{\mathrm{dry,c}}$ was also determined at SS = 1.51 % and observed to decrease from 123 nm to 103 nm over 7 h, corresponding to 2.9 ± 0.5 nm h^{-1}. However, it is notable that $D_{\mathrm{dry,c}}$ is larger at SS = 1.51 %, than at SS = 0.60 % and 1.02 %. This is more clearly seen in Fig. 3b, showing κ_{CCN} in the range 0.003–0.006 obtained at SS = 1.51 %, which is approximately a factor of ten smaller than the values obtained at 0.60 % and 1.02 %.

Tang et al. (2012) examined SOA from low initial concentrations of β-caryophyllene (5–20 ppb) and did not detect any temporal trends in the CCN activity of SOA generated in the absence of an OH scavenger. They consistently observed high κ_{CCN} values (0.13–0.25), ascribed to the low precursor concentrations resulting in SOA mainly composed of highly oxidized compounds of high hygroscopicity and CCN activity. This is consistent with the conclusions of Duplissy et al. (2008). It is notable, though, that the difference between 25 ppb (in the present study and that of Asa-Awuku et al., 2009) and 20 ppb (in Tang et al., 2012) cause more than a doubling in κ_{CCN} (from 0–0.06 at 25 ppb β-caryophyllene to 0.13–0.25, reported by Tang et al., 2012). Tang et al. (2012) reported lower κ_{CCN} for SOA generated in the presence of an OH scavenger beginning at 0.003 approximately 1 h after nucleation and increasing to > 0.1 after 10 h. Again, the higher values of κ_{CCN} were explained by the low initial precursor concentrations.

The CCN activity of particles generated with no lights on was related to volatility through the use of a TD. The effect for particles from experiments with the addition of an OH scavenger (experiments a and b) is seen in Fig. 4a: no relation between CCN activity and volatility was detected as no systematic change beyond experimental uncertainty was observed. However, κ_{CCN} values from the SD-CCNC were consistently higher than the data reported from the CF-CCNC. This could be caused by the two instruments operating at different supersaturations or due to effects of temperature, as suggested by Asa-Awuku et al. (2009). However, if the latter explanation is valid, it is puzzling that the TD does not appear to lower CCN activity as measured by the SD-CCNC. This could be due to differences in the residence times of the TD and in the growth chambers of the CCNCs, or the effect could be masked by the experimental uncertainties.

The effect of the TD on κ_{CCN} for particles from experiments without OH scavenger (experiments c–e) is illustrated in Fig. 4b. After passing through the TD set to a temperature of 35 or 50 °C (corresponding to 308 or 323 K, respectively), the CCN activity of the particles was lower, indicating that the volatile components evaporating from the surface in the TD were also the more hygroscopic. This is in agreement with previous observations for β-caryophyllene (Asa-Awuku et al., 2009; Alfarra et al., 2012; Tang et al., 2012). Only a small number of data points are available from the SD-CCNC. Therefore no firm conclusions can be drawn, but the SD-CCNC seemed to measure a slightly higher CCN activity than the CF-CCNC. Based on the effects of the TD on the measurements from the CF-CCNC, this was also expected since the CF-CCNC operated at a higher temperature: at $\mathrm{SS} = 0.77\,\%$ and ambient temperatures in the range 25–29 °C (298–302 K), the maximum temperature in the CF-CCNC was up to 43 °C (316 K), whereas during the experiments discussed in Fig. 4b the SD-CCNC operated at 21–27 °C (294–300 K).

The difference in the post-TD CCN activity indicates that the physical properties of the products from pure ozonolysis are different from those of SOA produced in the presence of OH. Either reactions without OH result in less variability in volatility and hygroscopicity, or else there is no connection between evaporative properties and CCN activity for the components generated from pure ozonolysis (i.e. when OH is scavenged).

4.2 CCN activity of particles generated in light experiments

In experiments f–l, ozonolysis of β-caryophyllene was carried out with lights turned on, either with or without the addition of HONO. SOA produced in this way was substantially more CCN active than SOA produced in experiments a–e (see Fig. 5). Figure 5a shows $D_{\mathrm{dry,c}}$ determined with the CF-CCNC as a function of time in experiments f and g (without HONO). For the three lowest supersaturations, the temporal trends were consistent with observations from the dark experiments: linear decreases in $D_{\mathrm{dry,c}}$ as functions of time were observed for supersaturations in the range of 0.25–0.35 % (see Table 2). $D_{\mathrm{dry,c}}$ measured at SS = 0.77 % also decreased with time, although a linear trend was not obvious. Figure 5b shows κ_{CCN} from experiments f and g; to make it more readable, error bars in κ_{CCN} are not shown. However, experimental errors were up to 30 %, (similar to the errors in κ_{CCN} shown in Fig. 3b).

Figure 5c shows $D_{\mathrm{dry,c}}$ as a function of time during experiments h–l (lighted ozonolysis with production of OH from photolysis of HONO). For three SS (0.29, 0.23, and 0.17 %), slight decreases in $D_{\mathrm{dry,c}}$ with time were observed (see Table 2), of the same order of magnitude as the decreases observed for SOA generated in experiments f and g. At the fourth SS (0.20 %), $D_{\mathrm{dry,c}}$ did not change with time. Figure 5d shows κ_{CCN} from experiments h–l (experimental errors up to 30 % not displayed). Within this relatively limited range of supersaturations (between 0.17 and 0.29 %), only a weak dependency of κ_{CCN} on SS was observed, as the average of κ_{CCN} determined at SS = 0.17 % was approximately 20 % lower than the average of κ_{CCN} measured at the three higher SS (0.059 versus 0.073, respectively).

Alfarra et al. (2012) studied SOA generated from photo-oxidation of β-caryophyllene in the presence of NO_x and determined κ_{GF} (using growth factors at 90 % relative humidity) as well as κ_{CCN}. They discovered no size dependency in hygroscopicity and little or no difference between the growth factors of individual particles at a measured dry size between 50 and 300 nm. Growth factors determined at a given particle size tended to increase slightly during an experiment, although not beyond experimental uncertainty, resulting in κ_{GF} in the range 0–0.03 and κ_{CCN} in the range 0–0.02. Alfarra et al. (2012) carried out photo-oxidation at two different initial β-caryophyllene concentrations, 50 and 250 ppb, but did not observe any influence of precursor concentration on hygroscopicity, which is in contrast with the findings for SOA generated from photo-oxidation of α-pinene by Duplissy et al. (2008) and the finding for β-caryophyllene by Tang et al. (2012). Considering that the formation and subsequent ageing of the SOA investigated by Alfarra et al. (2012) was only observed for up to 6 h, the magnitudes of κ_{GF} are in reasonable agreement with the measurements at 0.77 % in experiment g in the present study (Fig. 5b), which were also obtained within the first 6 h after initial nucleation.

Figure 6 shows the effect of sending particles through a TD prior to size selection and characterization in the two CCN counters. κ_{CCN} consistently increased with time independently of the TD temperature, and κ_{CCN} values from the CF-CCNC agreed well with values from the SD-CCNC. This is different from dark ozonolysis experiments, where particles were slightly less CCN active after passing them through the TD (see Fig. 4). These observations indicate that SOA generated under light exposure is not particularly volatile, or that the compounds contributing to the CCN activity are not highly volatile.

Figure 7 shows the effect of sending particles generated with lights on and the addition of HONO through a TD. All CF-CCNC data shown in Fig. 7 were obtained from three different experiments at SS = 0.29 %. The SD-CCNC data were obtained at a constant D_{dry} (100 and 150 nm) by varying SS, resulting in SS_c in the range 0.28–0.45 %. As was the case in Fig. 6, an increase in κ_{CCN} was observed for measurements from both the CF-CCNC and the SD-CCNC, but no effect was observed from the TD. κ_{CCN} measured with the CF-CCNC agreed with κ_{CCN} measured at 150 nm with the SD-CCNC. The κ_{CCN} values obtained with the SD-CCNC for 100 nm particles were, however, significantly higher. These data are associated with large uncertainties, but the difference may indicate a dependency of κ_{CCN} on SS (or $D_{dry,c}$).

4.3 Temperature effects

The CCN activity of SOA from oxidation of β-caryophyllene was characterized at several different supersaturations, and, as seen above, κ_{CCN} was not constant for all supersaturations. This is also shown in Fig. 8, which compiles data (without using the TD) from all smog chamber experiments. To guide the eye, a power function has been fit to the data. The trend and the scattering of data around the empirical fit was to some extent related to the effects of chemical ageing: when the CCN counters were operated at a constant SS for extended periods of time, an increase of κ_{CCN} was observed (see Figs. 3 and 5). Also, measurements at high values (> 1 %) were mainly performed during the first few hours after β-caryophyllene injection. Since chemical ageing resulted in a significant increase in CCN activity, it is also expected that the particles studied early in the experiment at high supersaturations were also the least CCN active. However, as clearly demonstrated in e.g. Fig. 3b, even for simultaneous measurements at different supersaturations, variations in κ_{CCN} are observed, and other explanations must exist.

The dependence of κ_{CCN} on SS may in part reflect the problems discussed by Petters and Kreidenweis (2007) of using a constant κ value for a wide range of concentrations: a single value of κ may not accurately characterize the water uptake of the aerosol for the whole atmospherically relevant range of humidity from sub- to supersaturation (Petters and Kreidenweis, 2007). κ-theory assumes that κ_{CCN} accounts for water activity, but deviations from ideality may vary significantly with dilution. Another possible explanation for the SS dependency of κ_{CCN} is based on the relation between SS and temperature in the CF-CCNC: for large SS, CF-CCNC operates at a high temperature (up to 51 °C, see Table 1) so that material may partially volatilize inside the instrument, leaving a residual that is less CCN active (assuming a previous correlation between volatility and CCN activity, as discussed by Asa-Awuku et al., 2009; Tang et al., 2012). Furthermore, material evaporating from the particle surface inside the CF-CCNC decreases the particle diameter to a value lower than selected by the DMA, resulting in a higher $\mathrm{SS_c}$. Such an effect has for example been observed for particles composed of pure glutaric acid (Frosch et al., 2010). However, if volatility was the only factor governing the change in κ_{CCN}, measurements performed with the SD-CCNC should consistently result in higher κ_{CCN} than measurements performed with the CF-CCNC. This is the case only for particles generated in experiments a–e (without exposure to light).

For particles generated under exposure to light, other explanations for the *SS* dependency of κ_{CCN} are suggested: for example, it was implicitly assumed that the chemical composition of SOA is independent of particle size. However, heterogeneous chemical reactions may play a role in chemical ageing, and the rates and products of such reactions might depend on particle size. Also, surface activity of products formed under dark and lighted conditions may differ. The κ_{CCN} values in the present study were calculated using a constant surface tension equal to the surface tension of pure water. However, using Köhler Theory Analysis (KTA) and filter sample extracts, Asa-Awuku et al. (2009) estimated that the hygroscopic fraction of SOA generated from ozonolysis of β-caryophyllene without exposure to light was surface active at activation conditions, resulting in $\sigma_{\mathrm{al}} = 65.5 \pm 2\,\mathrm{mN\,m^{-1}}$. Surface tension of products formed under lighted conditions has not yet been studied.

As shown by Li et al. (1998), Sorjamaa et al. (2004), and Prisle et al. (2008) it is important to account for a concentration dependence of surface tension and surfactant surface partitioning when calculating the CCN activity. Assuming a constant surface tension can lead to overestimation of the CCN activity (i.e. too high values of κ_{CCN}) in particular for small particles and high critical supersaturations. Detailed modeling accounting for surfactant partitioning is outside the scope of this work, however it is not likely that a reduced surface tension can explain the behavior observed in Fig. 8.

4.4 CCN activation kinetics

Growth kinetics of SOA particles is explored in Fig. 9, where the wet diameter of activated particles, D_{OPC}, is plotted as a function of $\mathrm{SS_c}$, both for ammonium sulphate particles (empirical fit from calibration data) and SOA. Error bars represent one standard deviation (described in Sect. 3.2). Rather than evaluating the absolute size of activated particles, the goal was to detect any differences between activated SOA and ammonium sulphate particles. D_{OPC} of SOA did not vary significantly from that of ammonium sulphate, implying that growth of β-caryophyllene SOA was not hindered.

Figure 10a–d shows D_{OPC} as a function of time after the initial injection of β-caryophyllene for different dry particle diameters. For comparison D_{OPC} of activating ammonium sulphate particles is also shown for the same critical supersaturation (solid, horizontal lines). No trend beyond experimental uncertainty was observed for dark and lighted ozonolysis (Fig. 10b–d), but for ozonolysis in the presence of an OH scavenger a slight increase in D_{OPC} was observed as a function of time.

In Fig. 10a, data for SS = 1.32 and 1.51 % were measured in two different experiments, and some discrepancies were observed. This could be due to small changes in experimental conditions, such as the ambient temperature, on which the temperature in the growth chamber of the CF-CCNC depends, or the number concentration of activated particles. This seems only relevant for SOA, since D_{OPC} for ammonium sulphate was measured on different days without any notable variation (see Fig. 1). The agreement between activation kinetics of SOA and ammonium sulphate is in contrast to the findings of Asa-Awuku et al. (2009), who observed an initial delay in activation kinetics followed by a subsequent increase, so that more than 6 h of chemical ageing were required for the growth kinetics of SOA particles to be comparable to those of ammonium sulphate. Since conditions such as precursor concentration, ozone levels, temperature and relative humidity in the smog chamber in experiments a–e were comparable to those presented by Asa-Awuku et al. (2009), it is surprising to find this contrast. Some variation in the present dataset may be masked by the error bars (one standard deviation was approximately 0.5–1 µm, corresponding to up to 30 %). As discussed above, daily variations in e.g. ambient and instrument temperatures could also affect the activation kinetics of SOA.

5 Conclusions

SOA generated from ozonolysis of β-caryophyllene and aged under exposure to various levels of OH radicals was characterized using two different CCN counters, one operating close to or below ambient room temperature and the other operating at higher temperatures (up to 51 °C). In all experiments, particles became progressively more CCN active when aged through exposure to OH and/or ozone. Fitting linear functions to κ_{CCN} as a function of time indicated that the increase was stronger for particles generated without exposure to light. κ_{CCN} depended heavily on exposure to OH. It was lower in experiments carried out in the presence of an OH scavenger ($\kappa_{\text{CCN}} < 0.006$ in experiments a–b) than in experiments with OH present (κ_{CCN} in the range 0.002–0.16 in the remaining experiments.), However, it is difficult to compare the different experiments, since CCN activity also depended on supersaturation in the CCN counters.

The TD data suggested that the CCN activity of SOA generated under dark conditions changed when SOA was exposed to temperatures of 35–50 °C, indicating that SOA contained semi-volatile material partially evaporating in the TD. This to some extent explained the supersaturation dependency of κ_{CCN}, as measured by the CF-CCNC, because the elevated temperature applied at high supersaturations potentially removed hygroscopic material from the particles. Other explanations involved a size dependency of the particle composition. Such effects are difficult to quantify, but could be examined further in future studies for example with online techniques, such as aerosol mass spectrometry or offline, through chemical characterization of filter samples. Investigation of CCN activation kinetics revealed that growth and activation of SOA particles were comparable to those of ammonium sulphate particles and therefore not kinetically hindered.

Acknowledgements. This work was supported by the EC project EUROCHAMP-2 and PEGASOS as well as the Swiss National Science Foundation.

References

Alfarra, M. R., Hamilton, J. F., Wyche, K. P., Good, N., Ward, M. W., Carr, T., Barley, M. H., Monks, P. S., Jenkin, M. E., Lewis, A. C., and McFiggans, G. B.: The effect of photochemical ageing and initial precursor concentration on the composition and hygroscopic properties of β-caryophyllene secondary organic aerosol, Atmos. Chem. Phys., 12, 6417–6436, doi:10.5194/acp-12-6417-2012, 2012.

Asa-Awuku, A. and Nenes, A.: Effect of solute dissolution kinetics on cloud droplet formation: extended Köhler theory, J. Geophys. Res., 112, 22201, doi:10.1029/2005JD006934, 2007.

Asa-Awuku, A., Engelhart, G. J., Lee, B. H., Pandis, S. N., and Nenes, A.: Relating CCN activity, volatility, and droplet growth kinetics of β-caryophyllene secondary organic aerosol, Atmos. Chem. Phys., 9, 795–812, doi:10.5194/acp-9-795-2009, 2009.

Asa-Awuku, A., Nenes, A., Gao, S., Flagan, R. C., and Seinfeld, J. H.: Water-soluble SOA from Alkene ozonolysis: composition and droplet activation kinetics inferences from analysis of CCN activity, Atmos. Chem. Phys., 10, 1585–1597, doi:10.5194/acp-10-1585-2010, 2010.

Bilde, M. and Svenningsson, B.: CCN activation of slightly soluble organics: the importance of small amounts of inorganic salt and particle phase, Tellus B, 56, 128–134, doi:10.1111/j.1600-0889.2004.00090.x, 2004.

Burtscher, H., Baltensperger, U., Bukowiecki, N., Cohn, P., Hüglin, C., Mohr, M., Matter, U., Nyeki, S., Schmatloch, V., Streit, N., and Weingartner, E.: Separation of volatile and non-volatile aerosol fractions by thermodesorption: instrumental development and applications, J. Aerosol Sci., 32, 427–442, doi:10.1016/S0021-8502(00)00089-6, 2001.

Chan, M. N., Surratt, J. D., Chan, A. W. H., Schilling, K., Offenberg, J. H., Lewandowski, M., Edney, E. O., Kleindienst, T. E., Jaoui, M., Edgerton, E. S., Tanner, R. L., Shaw, S. L., Zheng, M., Knipping, E. M., and Seinfeld, J. H.: Influence of aerosol acidity on the chemical composition of secondary organic aerosol from β-caryophyllene, Atmos. Chem. Phys., 11, 1735–1751, doi:10.5194/acp-11-1735-2011, 2011.

Donahue, N. M., Huff-Hartz, K. E., Chuong, B., Presto, A. A., Stanier, C. O., Rosenørn, T., Robinson, A. L., and Pandis, S. N.: Critical factors determining the variation in SOA yields from terpene ozonolysis: a combined experimental and computational study, Faraday Discuss., 130, 295–309, doi:10.1039/B417369D, 2005.

Duplissy, J., Gysel, M., Alfarra, M. R., Dommen, J., Metzger, A., Prevot, A. S. H., Weingartner, E., Laaksonen, A., Raatikainen, T., Good, N., Turner, S. F., McFiggans, G., and Baltensperger, U.: Cloud forming potential of secondary organic aerosol under near atmospheric conditions, Geophys. Res. Lett., 35, 03818, doi:10.1029/2007GL031075, 2008.

Engelhart, G. J., Asa-Awuku, A., Nenes, A., and Pandis, S. N.: CCN activity and droplet growth kinetics of fresh and aged monoterpene secondary organic aerosol, Atmos. Chem. Phys., 8, 3937–3949, doi:10.5194/acp-8-3937-2008, 2008.

Frosch, M., Zardini, A. A., Platt, S. M., Müller, L., Reinnig, M.-C., Hoffmann, T., and Bilde, M.: Thermodynamic properties and cloud droplet activation of a series of oxo-acids, Atmos. Chem. Phys., 10, 5873–5890, doi:10.5194/acp-10-5873-2010, 2010.

Frosch, M., Bilde, M., DeCarlo, P., Jurányi, Z., Tritscher, T., Dommen, J., Donahue, N. M., Gysel, M., Weingartner, E., Baltensperger, U.: Relating CCN activity and oxidation level of α-pinene secondary organic aerosol, J. Geophys. Res., 116, 22212, doi:10.1029/2011JD016401, 2011.

Gao, S., Keywood, M., Ng, N. L., Surratt, J., Varutbangkul, V., Bahreini, R., Flagan, R. C., and Seinfeld, J. H.: Low-molecular-weight and oligomeric components in secondary organic aerosol from the ozonolysis of cycloalkenes and alpha-pinene, J. Phys. Chem. A, 108, 10147–10164, doi:10.1021/jp047466e, 2004.

Goldstein, A. H. and Galbally, I. E.: Known and unexplored organic constituents in the Earth's atmosphere, Environ. Sci. Technol., 41, 1514–1521, doi:10.1021/es072476p, 2007.

Griffin, R. J., Cocker III, D. R., Seinfeld, J. H., and Dabdub, D.: Estimate of global atmospheric organic aerosol from oxidation of biogenic hydrocarbons, Geophys. Res. Lett., 26, 2721–2724, doi:10.1029/1999GL900476, 1999.

Guenther, A., Hewitt, N. C., Erickson, D., Fall, R., Geron, C., Graedel, T., Harley, P., Klinger, L., Lerdau, M., McKay, W. A., Pierce, T., Scholes, B., Steinbrecher, R., Tallamraju, R., Taylor, J., and Zimmerman, P.: A global model of natural volatile organic compound emissions, J. Geophys. Res., 100, 8873–8892, doi:10.1029/94JD02950, 1995.

Hallquist, M., Wenger, J. C., Baltensperger, U., Rudich, Y., Simpson, D., Claeys, M., Dommen, J., Donahue, N. M., George, C., Goldstein, A. H., Hamilton, J. F., Herrmann, H., Hoffmann, T., Iinuma, Y., Jang, M., Jenkin, M. E., Jimenez, J. L., Kiendler-Scharr, A., Maenhaut, W., McFiggans, G., Mentel, Th. F., Monod, A., Prévôt, A. S. H., Seinfeld, J. H., Surratt, J. D., Szmigielski, R., and Wildt, J.: The formation, properties and impact of secondary organic aerosol: current and emerging issues, Atmos. Chem. Phys., 9, 5155–5236, doi:10.5194/acp-9-5155-2009, 2009.

Hoffmann, T., Odum, J. R., Bowman, F., Collins, D., Klockow, D., Flagan, R. C., and Seinfeld, J. H.: Formation of organic aerosols from the oxidation of biogenic hydrocarbons, J. Atmos. Chem., 26, 189–222, doi:10.1023/A:1005734301837, 1997.

Huff-Hartz, K. E, Rosenørn, T., Ferchak, S. R., Raymond, T. M., Bilde, M., Donahue, N. M., and Pandis, S. N.: Cloud condensation nuclei activation of monoterpene and sesquiterpene secondary organic aerosol, J. Geophys. Res., 110, 14208, doi:10.1029/2004jd005754, 2005.

IPCC: Climate Change 2007: The Physical Science Basis. Contribution of Working Group I to the Fourth Assessment Report of the Intergovernmental Panel on Climate Change, Cambridge University Press, Cambridge, UK, 2007.

Jang, M. and Kamens, R. M.: Atmospheric secondary aerosol formation by heterogeneous reactions of aldehydes in the presence of a sulfuric acid aerosol catalyst, Environ. Sci. Technol., 35, 4758–4766, doi:10.1021/es010790s, 2001.

Jaoui, M., Leungsakul, S., and Kamens, R. M.: Gas and particle products distribution from the reaction of β-caryophyllene with ozone, J. Atmos. Chem., 45, 261–287, doi:10.1023/A:1024263430285, 2003.

Jimenez, J. L., Canagaratna, M. R., Donahue, N. M., Prevot, A. S. H., Zhang, Q., Kroll, J. H., DeCarlo, P. F., Allan, J. D., Coe, H., Ng, N. L., Aiken, A. C., Docherty, K. S., Ulbrich, I. M., Grieshop, A. P., Robinson, A. L., Duplissy, J., Smith, J. D., Wilson, K. R., Lanz, V. A., Hueglin, C., Sun, Y. L., Tian, J., Laaksonen, A., Raatikainen, T., Rautiainen, J., Vaattovaara, P., Ehn, M., Kulmala, M., Tomlinson, J. M., Collins, D. R., Cubison, M. J., Dunlea, E. J., Huffman, J. A., Onasch, T. B., Alfarra, M. R., Williams, P. I., Bower, K., Kondo, Y., Schneider, J., Drewnick, F., Borrmann, S., Weimer, S., Demerjian, K., Salcedo, D., Cottrell, L., Griffin, R., Takami, A., Miyoshi, T., Hatakeyama, S., Shimono, A., Sun, J. Y., Zhang, Y. M., Dzepina, K., Kimmel, J. R., Sueper, D., Jayne, J. T., Herndon, S. C., Trimborn, A. M., Williams, L. R., Wood, E. C., Middlebrook, A. M., Kolb, C. E., Baltensperger, U., and Worsnop, D. R.: Evolution of organic aerosols in the atmosphere, Science, 326, 1525–1529, doi:10.1126/science.1180353, 2009.

Jurányi, Z., Gysel, M., Duplissy, J., Weingartner, E., Tritscher, T., Dommen, J., Henning, S., Ziese, M., Kiselev, A., Stratmann, F., George, I., and Baltensperger, U.: Influence of gas-to-particle partitioning on the hygroscopic and droplet activation behaviour of alpha-pinene secondary organic aerosol, Phys. Chem. Chem. Phys., 11, 8091–8097, doi:10.1039/B904162A, 2009.

Kanakidou, M., Seinfeld, J. H., Pandis, S. N., Barnes, I., Dentener, F. J., Facchini, M. C., Van Dingenen, R., Ervens, B., Nenes, A., Nielsen, C. J., Swietlicki, E., Putaud, J. P., Balkanski, Y., Fuzzi, S., Horth, J., Moortgat, G. K., Winterhalter, R., Myhre, C. E. L., Tsigaridis, K., Vignati, E., Stephanou, E. G., and Wilson, J.: Organic aerosol and global climate modelling: a review, Atmos. Chem. Phys., 5, 1053–1123, doi:10.5194/acp-5-1053-2005, 2005.

Kleindienst, T. E., Jaoui, M., Lewandowski, M., Offenberg, J. H., Lewis, C. W., Bhave, P. V., and Edney, E. O.: Estimates of the contributions of biogenic and anthropogenic hydrocarbons to secondary organic aerosol at a Southeastern US location, Atmos. Environ., 41, 8288–8300, doi:10.1016/j.atmosenv.2007.06.045, 2007.

Köhler, H.: The nucleus in and the growth of hygroscopic droplets, T. Faraday Soc., 32, 1152–1161, doi:10.1039/TF9363201152, 1936.

Kuwata, M., Chen, Q., and Martin, S. T.: Cloud Condensation Nuclei (CCN) activity and oxygen-to-carbon elemental ratios following thermodenuder treatment of organic particles grown by α-pinene ozonolysis, Phys. Chem. Chem. Phys., 13, 14571–14583, doi:10.1039/c1cp20253g, 2011.

Lance, S., Medina, J., Smith, J. N., and Nenes, A.: Mapping the operation of the DMT continuous flow CCN counter, Aerosol Sci. Tech., 40, 242–254, doi:10.1080/02786820500543290, 2006.

Lathem, T. L. and Nenes, A.: Water vapor depletion in the DMT continuous-flow CCN chamber: effects on supersaturation and droplet growth, Aerosol Sci. Tech., 45, 604–615, doi:10.1080/02786826.2010.551146, 2011.

Lee, A., Goldstein, A. H., Keywood, M. D., Gao, S., Varutbangkul, V., Bahreini, R., Ng, N. L., Flagan, R. C., and Seinfeld, J. H.: Gas-phase products and secondary aerosol yields from the ozonolysis of ten different terpenes, J. Geophys. Res., 111, 07302, doi:10.1029/2005jd006437, 2006.

Li, Z., Williams, A. L., and Rood, M. J.: Influence of soluble surfactant properties on the activation of aerosol particles containing inorganic solute, J. Atmos. Sci., 55, 1859–1866, doi:10.1175/1520-0469(1998)055<1859:IOSSPO>2.0.CO;2, 1998.

Nenes, A., Ghan, S., Abdul-Razzak, H., Chuang, P. Y., and Seinfeld, J. H.: Kinetic limitations on cloud droplet formation and impact on cloud albedo, Tellus B, 53, 133–149, doi:10.1034/j.1600-0889.2001.d01-12.x, 2001.

Paulsen, D., Dommen, J., Kalberer, M., Prévôt, A. S. H., Richter, R., Sax, M., Steinbacher, M., Weingartner, E., and Baltensperger, U.: Secondary organic aerosol formation by irradiation of 1,3,5-trimethylbenzene-NO_x-H_2O in a new reaction chamber for atmospheric chemistry and physics, Environ. Sci. Technol., 39, 2668–2678, doi:10.1021/es0489137, 2005.

Petters, M. D. and Kreidenweis, S. M.: A single parameter representation of hygroscopic growth and cloud condensation nucleus activity, Atmos. Chem. Phys., 7, 1961–1971, doi:10.5194/acp-7-1961-2007, 2007.

Prenni, A. J., Petters, M. D., Kreidenweis, S. M., DeMott, P. J., and Ziemann, P. J. : cloud droplet activation of secondary organic aerosol, J. Geophys. Res., 112, 10223, doi:10.1029/2006jd007963, 2007.

Prisle, N. L., Raatikainen, T., Sorjamaa, R., Svenningsson, B., Laaksonen, A., and Bilde, M.: Surfactant partitioning in cloud droplet activation: a study of C8, C10, C12 and C14 normal fatty acid sodium salts, Tellus B, 60, 416–431, doi:10.1111/j.1600-0889.2008.00352.x, 2008.

Raatikainen, T., Moore, R. H., Lathem, T. L., and Nenes, A.: A coupled observation – modeling approach for studying activation kinetics from measurements of CCN activity, Atmos. Chem. Phys., 12, 4227–4243, doi:10.5194/acp-12-4227-2012, 2012.

Riipinen, I. Pierce, J. R., Donahue, N. M., and Pandis, S. N.: Equilibration time scales of organic aerosol inside thermodenuders: evaporation kinetics versus thermodynamics, Atmos. Environ., 44, 597–607, doi:10.1016/j.atmosenv.2009.11.022, 2010.

Rissler, J., Vestin, A., Swietlicki, E., Fisch, G., Zhou, J., Artaxo, P., and Andreae, M. O.: Size distribution and hygroscopic properties of aerosol particles from dry-season biomass burning in Amazonia, Atmos. Chem. Phys., 6, 471–491, doi:10.5194/acp-6-471-2006, 2006.

Roberts, G. C. and Nenes, A.: A continuous-flow streamwise thermal-gradient CCN chamber for atmospheric measurements, Aerosol Sci. Technol., 39, 206–221, doi:10.1080/027868290913988, 2005.

Sakulyanontvittaya, T., Guenther, A., Helmig, D., Milford, J., and Wiedinmyer, C.: Secondary organic aerosol from sesquiterpene and monoterpene emissions in the United States, Environ. Sci. Technol., 42, 8784–8790, doi:10.1021/es800817r, 2008.

Seinfeld, J. H. and Pandis, S. N.: Atmospheric Chemistry and Physics. From Air Pollution to Climate Change, 2nd edition, Wiley Interscience Publications, John Wiley & Sons, New York, 2006.

Sjogren, S., Gysel, M., Weingartner, E., Baltensperger, U., Cubison, M. J., Coe, H., Zardini, A. A., Marcolli, C., Krieger, U. K., and Peter, T.: Hygroscopic growth and water uptake kinetics of two-phase aerosol particles consisting of ammonium sulfate, adipic and humic acid mixtures, J. Aerosol Sci., 38, 157–171, doi:10.1016/j.jaerosci.2006.11.005, 2007.

Snider, J. R., Petters, M. D., Wechsler, P., and Liu, P. S. K.: Supersaturation in the Wyoming CCN instrument, J. Atmos. Ocean. Tech., 23, 1323–1339, doi:10.1175/JTECH1916.1, 2006.

Snider, J. R., Wex, H., Rose, D., Kristensson, A., Stratmann, F., Hennig, T., Henning, S., Kiselev, A., Bilde, M., Burkhart, M., Dusek, U., Frank, G. P., Kiendler-Scharr, A., Mentel, T. F., Petters, M. D. and Pöschl, U.: Intercomparison of cloud condensation nuclei and hygroscopic fraction measurements: coated soot particles investigated during the LACIS Experiment in November (LExNo), J. Geophys. Res., 115, 11205, doi:10.1029/2009JD012618, 2010.

Sorjamaa, R., Svenningsson, B., Raatikainen, T., Henning, S., Bilde, M., and Laaksonen, A.: The role of surfactants in Köhler theory reconsidered, Atmos. Chem. Phys., 4, 2107–2117, doi:10.5194/acp-4-2107-2004, 2004.

Svenningsson, B. and Bilde, M.: Relaxed step functions for evaluation of CCN counter data on size-separated aerosol particles, J. Aerosol Sci., 39, 592–608, doi:10.1016/j.jaerosci.2008.03.004, 2008.

Taira, M. and Kanda, Y.: Continuous generation system for low-concentration gaseous nitrous acid, Anal. Chem., 62, 630–633, doi:10.1021/ac00205a018, 1990.

Tang, X., Cocker III, D. R., and Asa-Awuku, A.: Are sesquiterpenes a good source of secondary organic cloud condensation nuclei (CCN)? Revisiting β-caryophyllene CCN, Atmos. Chem. Phys. Discuss., 12, 8547–8577, doi:10.5194/acpd-12-8547-2012, 2012.

Tritscher, T., Dommen, J., DeCarlo, P. F., Gysel, M., Barmet, P. B., Praplan, A. P., Weingartner, E., Prévôt, A. S. H., Riipinen, I., Donahue, N. M., and Baltensperger, U.: Volatility and hygroscopicity of aging secondary organic aerosol in a smog chamber, Atmos. Chem. Phys., 11, 11477–11496, doi:10.5194/acp-11-11477-2011, 2011.

Wex, H., Hennig, T., Salma, I., Ocskay, R., Kiselev, A., Henning, S., Massling, A., Wiedensohler, A., and Stratmann, F.: Hygroscopic growth and measured and modeled critical super-saturations of an atmospheric HULIS sample, Geophys. Res. Lett., 34, 02818, doi:10.1029/2006GL028260, 2007.

Table 1. Summary of all experiments. Four types of experiments have been carried out: dark ozonolysis with OH scavenger (2-butanol); dark ozonolysis (without OH scavenger); lighted ozonolysis; lighted ozonolysis with HONO (OH-source). Also shown are the ranges of $D_{\text{dry,c}}$ and SS_c studied with the CF-CCNC, as well as the ambient temperature (T_{am}) and the maximum temperature in the CF-CCNC ($T_{\text{CF,max}}$) for each individual experiment.

	Date	$D_{\text{dry,c}}$ nm	SS_c(CF-CCNC) %	T_{am} °C	$T_{\text{CF,max}}$ °C
1: dark ozonolysis + OH scavenger					
a	26 May	122–163	1.32–1.51	28–30	47–51
b	2 Jun	114–190	1.32–1.51	24–26	42–48
2: dark ozonolysis					
c	5 May	47–222	0.15–1.45	24–26	31–46
d	20 May	112–129	0.77	25–29	39–43
e	12 Jun	99–159	1.32–1.66	27–28	48–50
3: ozonolysis of β-caryophyllene + light					
f	22 May	76–144	0.29–0.77	27–30	34–41
g	8 Jun	87–157	0.25–0.77	26–28	32–40
4: ozonolysis of β-caryophyllene + HONO + light					
h	4 Jun	122–218	0.17–1.74	25–28	31–51
i	10 Jun	101–205	0.17–0.60	25–29	32–38
j	15 Jun	60–223	0.17–1.51	25–28	33–48
k	17 Jun	122–222	0.17–0.77	25–30	35–39
l	19 Jun	100–170	0.45–1.89	26–29	38–51

Table 2. Effect of ageing on $D_{\mathrm{dry,c}}$ at various supersaturations in the four types of smog chamber experiments.

Present study		Asa-Awuku et al. (2009)	
SS/%	d $D_{\mathrm{dry,c}}$/d time	SS/%	d $D_{\mathrm{dry,c}}$/d time
1: dark ozonolysis + OH scavenger			
1.51	$2.8 \pm 0.16\,\mathrm{nm\,h^{-1}}$	–	–
1.32	$3.0 \pm 0.2\,\mathrm{nm\,h^{-1}}$	–	–
–	–	1.02	$3.0\,\mathrm{nm\,h^{-1}}$
–	–	0.61	$2.0\,\mathrm{nm\,h^{-1}}$
2: dark ozonolysis			
1.51	$2.9 \pm 0.5\,\mathrm{nm\,h^{-1}}$	–	–
1.02	$0.85 \pm 0.09\,\mathrm{nm\,h^{-1}}$	1.02	$2.8\,\mathrm{nm\,h^{-1}}$
0.60	$3.3 \pm 0.3\,\mathrm{nm\,h^{-1}}$	0.61	$2.6\,\mathrm{nm\,h^{-1}}$
3: ozonolysis of β-caryophyllene + light			
0.35	$0.54 \pm 0.2\,\mathrm{nm/h}$	–	–
0.29	$0.59 \pm 0.14\,\mathrm{nm\,h^{-1}}$	–	–
0.25	$1.16 \pm 0.3\,\mathrm{nm\,h^{-1}}$	–	–
4: ozonolysis of β-caryophyllene + HONO + light			
0.29	$0.69 \pm 0.12\,\mathrm{nm\,h^{-1}}$	–	–
0.23	$0.47 \pm 0.2\,\mathrm{nm\,h^{-1}}$	–	–
0.20	$0.23 \pm 0.3\,\mathrm{nm\,h^{-1}}$	–	–
0.17	$0.78 \pm 0.4\,\mathrm{nm\,h^{-1}}$	–	–

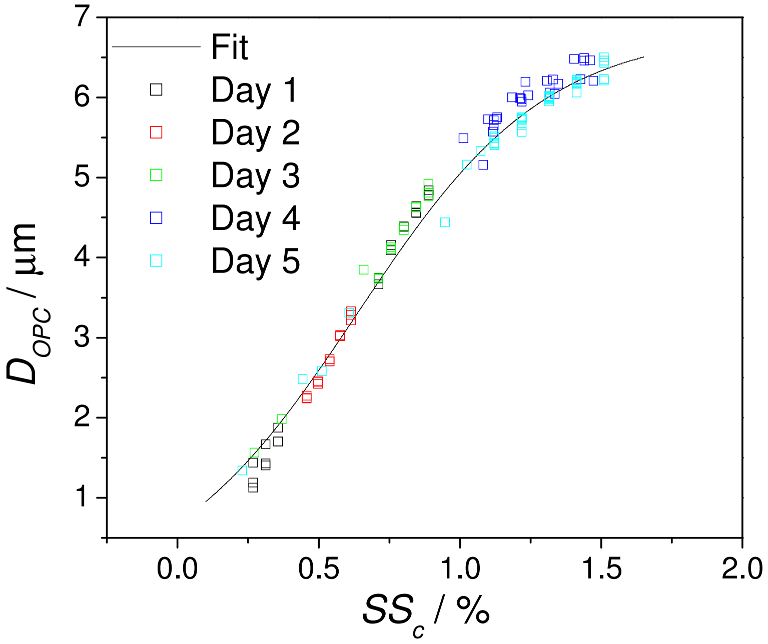

Fig. 1. Diameter of activated ammonium sulphate particles (D_{OPC}) as a function of critical supersaturation ($\mathrm{SS_c}$). An empirical fit is also shown ($y = 1.24 - 2.79 \cdot x + 16.82 \cdot x^2 - 13.70 \cdot x^3 + 3.50 \cdot x^4$).

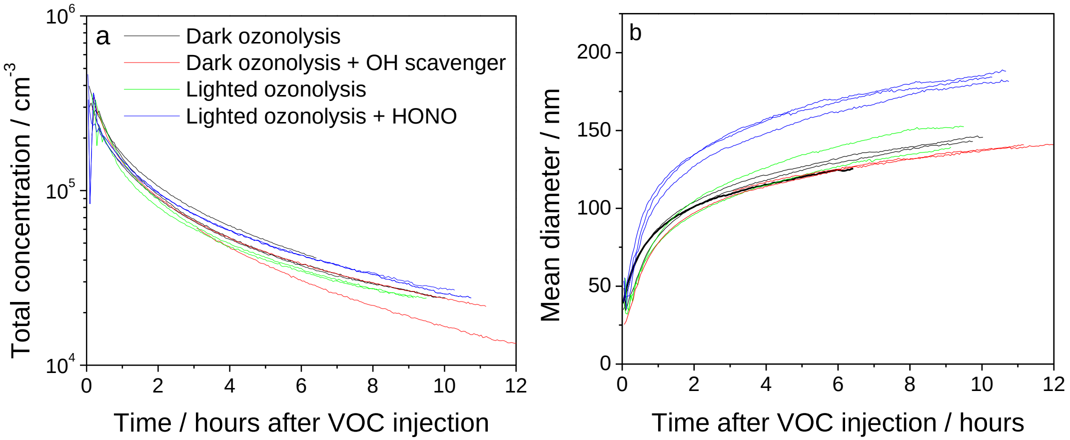

Fig. 2. Total number concentration **(a)** and mean diameter **(b)** of particles produced in individual experiments (the four types of experiments are summarized in Table 1) as a function of time. Note that data were not corrected for losses to the smog chamber walls.

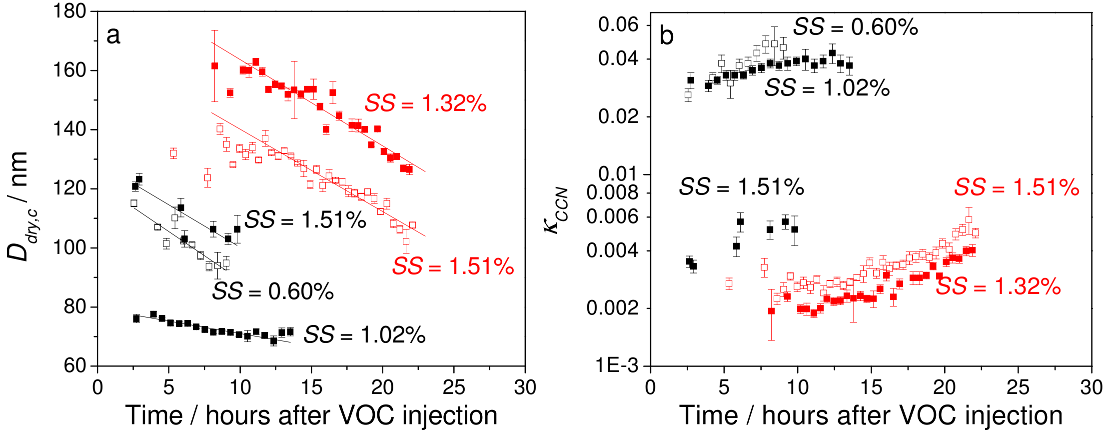

Fig. 3. Critical diameter $D_{\mathrm{dry,c}}$ **(a)** and κ_{CCN} **(b)** of SOA formed from dark ozonolysis of β-caryophyllene measured with the CF-CCNC, either without (black points/lines) or with (red points/lines) the addition of an OH scavenger (2-butanol). Data are shown for different supersaturations in the range 0.60–1.51 %. For each supersaturation, a straight line (see Table 2) is fitted to $D_{\mathrm{dry,c}}$.

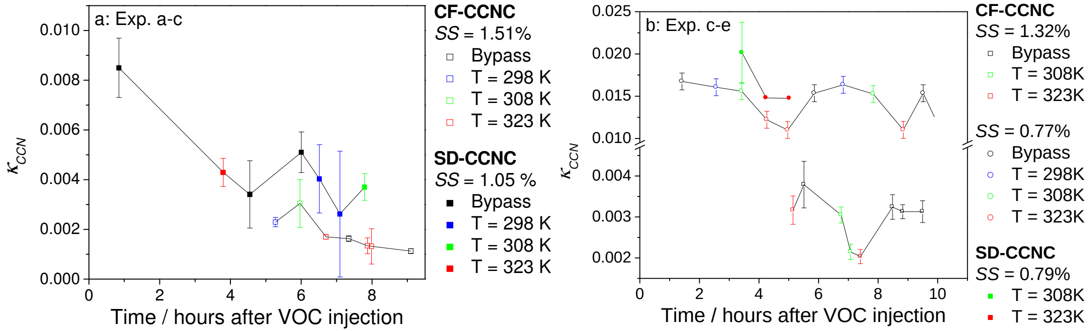

Fig. 4. Single hygroscopicity parameters (κ_{CCN}) for SOA from dark ozonolysis of β-caryophyllene with **(a)** or without **(b)** the addition of an OH scavenger (2-butanol). For some time during each experiment, the aerosol particles were sent through a thermodenuder, operated at three different temperatures. Points are connected to aid visual inspection.

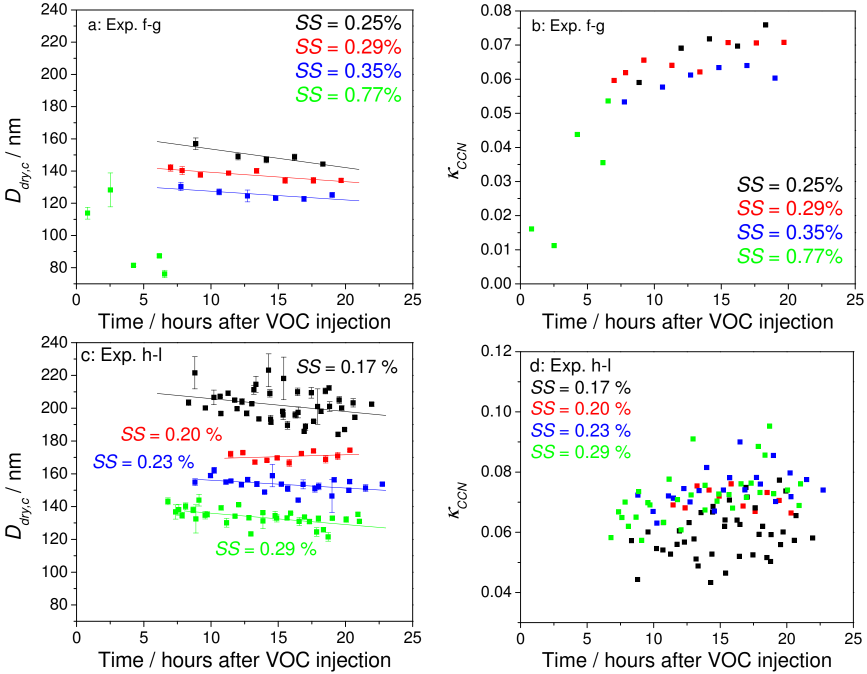

Fig. 5. Critical diameter ($D_{\mathrm{dry,c}}$) and κ_{CCN} of SOA measured with the CF-CCNC for experiments with lights on (**a** and **b**) and with lights on and the addition of HONO (**c** and **d**). Data are shown for different supersaturations in the range 0.17–0.77 %. Experimental uncertainties in determining κ_{CCN} were up to 30 % (error bars not shown). Straight lines were fitted to $D_{\mathrm{dry,c}}$ (see Table 2).

Title Page
Abstract Introduction
Conclusions References
Tables Figures
|◀ ▶|
◀ ▶
Back Close
Full Screen / Esc
Printer-friendly Version
Interactive Discussion

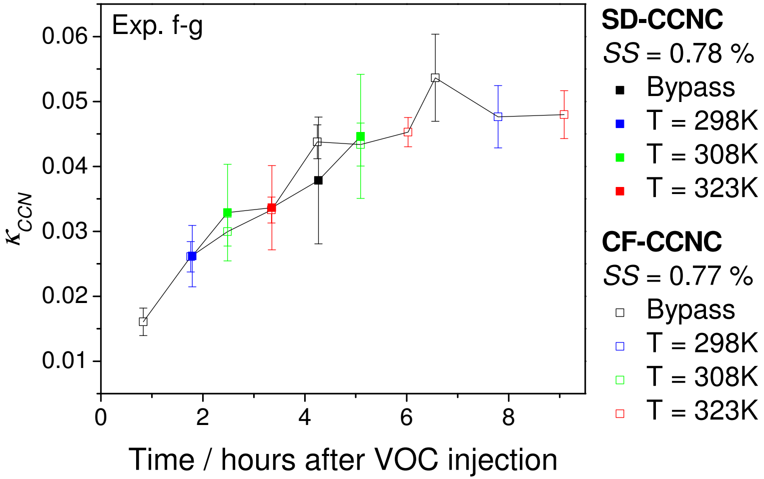

Fig. 6. Single hygroscopicity parameters (κ_{CCN}) of SOA from lighted ozonolysis of β-caryophyllene. For some time during each experiment, the aerosol particles were sent through a thermodenuder, operated at three different temperatures. Points are connected to aid visual inspection.

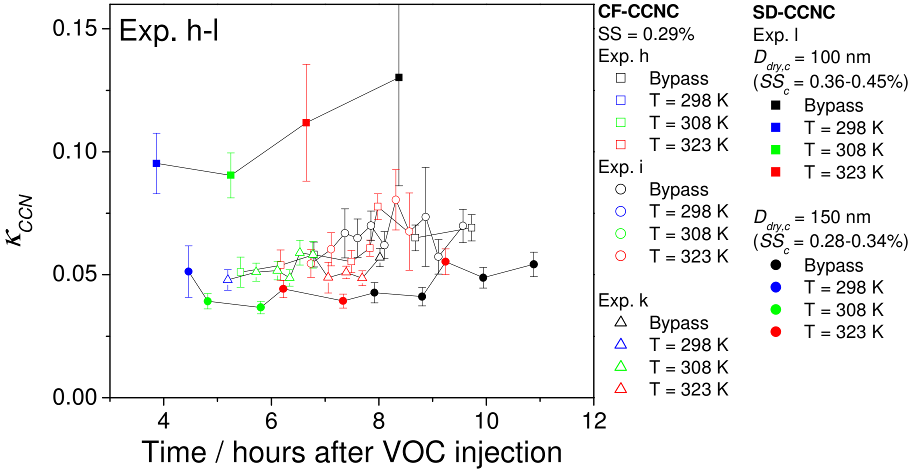

Fig. 7. Single hygroscopicity parameter (κ_{CCN}) of SOA formed from ozonolysis of β-caryophyllene with the addition of OH (generated from photolysis of HONO). For some time during each experiment, the aerosol particles were sent through a thermodenuder operated at three different temperatures. Points are connected to aid visual inspection.

Title Page
Abstract | Introduction
Conclusions | References
Tables | Figures
◀▮ | ▶▮
◀ | ▶
Back | Close
Full Screen / Esc
Printer-friendly Version
Interactive Discussion

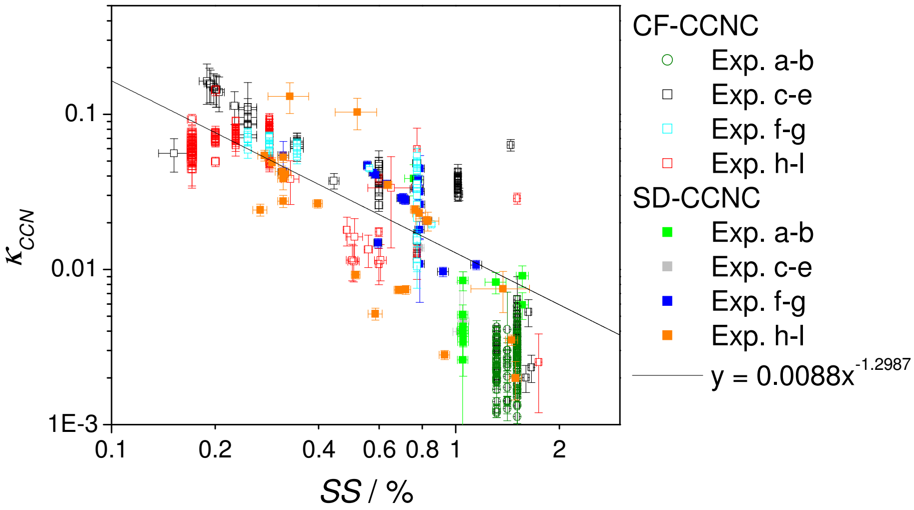

Fig. 8. Single hygroscopicity parameter (κ_{CCN}) of SOA as a function of supersaturation for the four different types of experiments described in Table 1. To guide the eye, all available data are compared to a power law fit (empirical fit).

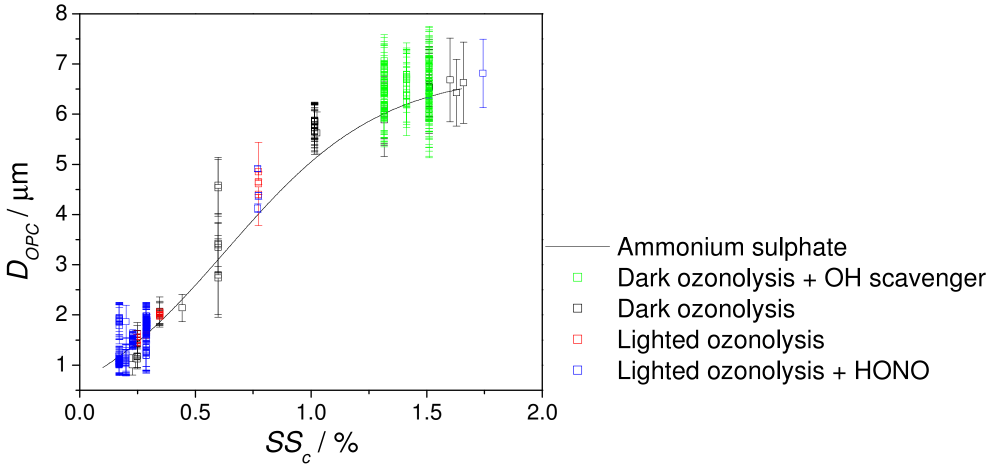

Fig. 9. Diameter of activated particles (D_{OPC}) as a function of critical supersaturation (SS_c). The individual points from smog chamber experiments are compared to the curve obtained from ammonium sulphate calibrations (see Fig. 1).

Title Page
Abstract | Introduction
Conclusions | References
Tables | Figures
◀| |▶
◀ ▶
Back | Close
Full Screen / Esc
Printer-friendly Version
Interactive Discussion

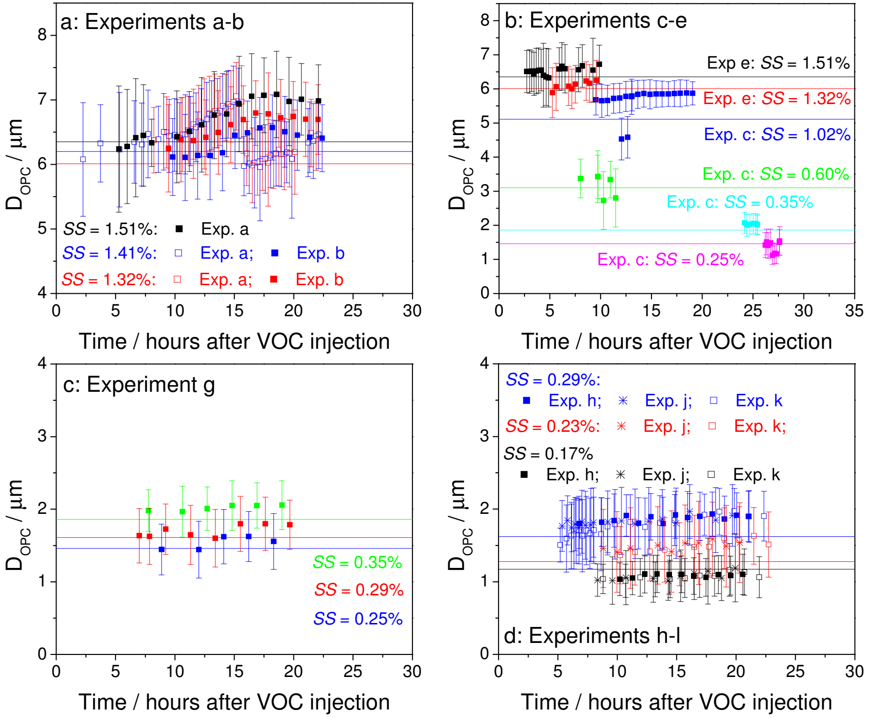

Fig. 10. Diameter of activated particles (D_{OPC}) as a function of time after injection of β-caryophyllene for different particle sizes, compared to D_{OPC} of activating ammonium sulphate particles with the same critical supersaturation (solid, horizontal lines). Data are separated into dark ozonolysis with OH scavenger **(a)**, dark ozonolysis **(b)**, lighted ozonolysis **(c)** and lighted ozonolysis with HONO **(d)**.